Polymer Degradation and Stability 193 (2021) 109726

Contents lists available at ScienceDirect

Polymer Degradation and Stability

journal homepage: www.elsevier.com/locate/polymdegradstab

Novel poly(azoamide triazole)s containing twin azobenzene units in the backbone. Synthesis, characterization, and *in vitro* degradation studies

Adrián Suárez-Cruz, Inmaculada Molina-Pinilla, Khalid Hakkou, Cristian Rangel-Núñez, Manuel Bueno-Martínez*

Departamento de Química Orgánica y Farmacéutica. Facultad de Farmacia. Universidad de Sevilla, C/ Profesor García González 2, 41012 Sevilla, Spain

ARTICLE INFO

Article history:
Received 5 June 2021
Revised 15 September 2021
Accepted 19 September 2021
Available online 28 September 2021

Keywords:
Click polymerization
Degradable polymer
Azo polymer
Azobenzene
Dithionite reduction
Biodegradable polymer

ABSTRACT

We describe the synthesis and characterization of four new light and reduction sensitives poly(azoamide triazole)s, in which the azobenzene units are found along the main chain of the macromolecule. These polymers were prepared by the azide-alkyne cycloaddition reaction catalyzed with copper (I) (CuAAC). They were obtained in high yield and with apparent molecular weights in the range from 95 to 148 kDa. All poly(azoamide triazole)s are soluble in polar aprotic solvents, and two of them are also soluble in chloroform showing good coating and film-forming properties. They were characterized by Fourier transform infrared, nuclear magnetic resonance (NMR), ultraviolet-visible spectroscopy and gel permeation chromatography (GPC). The photoisomerization study of the synthesized polymers has been carried out by UV–Vis spectroscopy, as well as their *trans-cis-trans* reversibility behavior. Differential scanning calorimetry (DSC) and themogravimetric analysis (TGA) were used to investigate their thermal properties. Results show that the polymers were amorphous and stable up to 300 °C under nitrogen. The hydrolytic degradation of films of these polymers has been studied *in vitro* under various conditions of pH and temperature and was monitored by GPC. Furthermore, the presence of azo units along the polymer backbone as cleavable groups provides access to their degradation by reduction. In this sense, the degradation of polymers has also been studied using sodium dithionite as a mimic of the enzyme azoreductase. The results of these studies show that the polymers are stable enough under hydrolytic physiological conditions, but they degrade rapidly when sodium dithionite is used. A preliminary study of biocompatibility of polymers **PAAT1** and **PAAT4** has been carried out. A hemolysis study with human red blood cells (hRBC) and a cytotoxicity study with human gingival fibroblasts (HGnF) have been carried out. The results obtained suggest that these polymers could be good candidates to be used as drug coating materials.

1. Introduction

The design and preparation of drug delivery systems that allow the release of bioactive compounds in a controlled and localized way have received a great deal of attention in recent decades. These systems, which were initially sensitive to a particular stimulus, such as light, pH, oxidizing or reducing conditions, certain enzymes, or temperature [1–9], have been the basis to develop systems that respond to dual or multiple signals, such as redox and pH [10], temperature and pH [11], temperature and enzyme [12], reducing conditions and light [13], enzyme and pH [14–16]; light and pH [17–19]; light and enzyme [20] and others [21].

Azo derivatives have been widely used for several applications, for example, as surfactants [22], gelators [23], liquid crystals [24] or biocides [25]. Azobenzene derivatives have also been used for the preparation of stimulus-sensitive drug delivery systems based on their photochemical behavior [26]. As it is well known, azobenzenes are photosensitive chromophores that have an unique sensitivity to light (or heat), which causes reversible *trans-cis* photoisomerization [27] leading to significant changes in their molecular size and dipole moments [28]. This photoisomerization process can also have an impact on other characteristics of the azo group, such as its sensitivity to reduction. Boulègue and collaborators have observed an increase in the reduction rate of *cis*

* Corresponding author.
E-mail address: mbueno@us.es (M. Bueno-Martínez).

https://doi.org/10.1016/j.polymdegradstab.2021.109726

azobenzene in relation to the *trans* isomer [29], which may allow a greater control of the degradation of this type of material.

There are a wide variety of applications in biomedicine that use the sensitivity of azo polymers to light and reduction [14,30–38]. Although azobenzene derivatives can also be used in any tumor tissue that suffers from hypoxic conditions or that expresses azoreductases, as for example, in the case of liver cancer cells [39], we are interested in their use in the design and preparation of systems that allow the vectorization of drugs to the colon through oral administration. Many compounds containing azobenzene in their structure have been studied for enabling oral administration and colonic release of specific drugs. Thus, various non-polymeric prodrugs [40–44], as well as macromolecular prodrugs which contain the azo group in the main or side chain, have been developed [45–53]. The bioactive compounds can be protected by polymeric coatings or matrixes based on azobenzene to reach the colonic delivery. In seminal work, Saffran and coworkers first used this approach for oral administration of azo polymer-coated peptide drugs [54]. In this way, drugs are protected from the adverse environmental conditions faced by these bioactive compounds in the gastrointestinal tract, delaying the release until the combination of azo-derivative materials and drugs reaches the colon. Azo compounds degrade in the colon because microbiome excretes the enzyme azoreductase, which can reduce selectively the azobenzene group to aromatic amines [36,55–57]. Although azoreductase enzymes have the most suitable characteristics to carry out the reduction of azo group, managing this type of enzyme at laboratory conditions can be difficult and results heavily depend on the gene codification of the enzyme. For this reason, other non-biological compounds such as hydrazine hydrate [58,59] or sodium dithionite [30,31,35,60,61] can be used for the same purpose. In particular, it is common to find the use of sodium dithionite since this reducing agent acts in a gentle way, it is cheap and potentially bioorthogonal [38].

The design of azo polymers that exhibit adequate sensitivity under biological and chemical conditions is an important research objective with implications in different fields. We previously reported on the synthesis of linear copoly(azoester triazole)s containing different amounts of the prodrug olsalazine in the polymer backbone [53]. Herein, we describe the synthesis and characterization of four new light and reduction sensitive poly(azoamide triazole)s, in which the azo units are found along the main chain of the macromolecule. These polymers were prepared by the azide-alkyne cycloaddition reaction catalyzed with copper (I) (CuAAC). The hydrolytic degradation of these polymers has been studied under various conditions of pH and temperature. Likewise, the degradation using sodium dithionite as a mimic of the enzyme azoreductase has also been studied.

2. Material and methods

2.1. Materials

All solvents and reagents were obtained from Merck and were used without further purification. 96-wells plates, Petri dishes, bovine fetal serum, Dulbecco's Modified Eagle's Medium, antibiotics, phosphate buffered saline (PBS) and trypsin were obtained from Thermo Fisher Scientific (Massachusetts, USA). Human gingival fibroblasts were purchased from Innoprot (Vizcaya, Spain).

2.2. Measurements

Thin-layer chromatography (TLC) was performed on Silica Gel 60 F254 (E. Merck) with detection by UV light or charring with H_2SO_4 or phosphomolybdic acid. Flash column chromatography was performed using E. Merck Silica Gel 60 (230–400 mesh). Fourier transform infrared (FTIR) spectra were recorded on a JASCO FT/IR-4200 spectrometer in the wavenumber range from 650 to 4000 cm^{-1} using films or KBr disks. ^1H and ^{13}C NMR spectra were recorded in the CITIUS of the Universidad de Sevilla using a Bruker AV300, Bruker AMX-500 or Bruker AVIII-700 spectrometers. Chemical shifts are reported as parts per million (ppm) and are referenced to the residual solvent signals as the internal standard. Two-dimensional ^1H–^1H homonuclear and ^{13}C-^1H heteronuclear shift correlation spectra were recorded with the COSY and HETCOR pulse sequences, respectively.

Elemental analyses were carried out in the Microanalysis Laboratories of the CITIUS Service at the Universidad de Sevilla. Chemical ionization (CI) and fast-atom bombardment mass spectra were performed on a Micromass Autospec spectrometer. FABMS spectra were obtained using thioglycerol-NaI as a matrix. The thermal behavior of the polymers was examined by differential scanning calorimetry (DSC) using a TA DSC Q200 Instrument, calibrated with indium. Samples of about 2–3 mg were heated at a rate of 10 °C/min under a nitrogen flow rate of 20 mL/min and cooled to −35 °C. Thermogravimetric analyses (TGA) were carried out by a SDT Q600 TA instrument at a heating rate of 10 °C/min under a nitrogen flow of 100 mL/min, and the temperature range was from room temperature to 600 °C. The size exclusion chromatography instrument consisted of a Waters apparatus equipped with a Waters 2414 refractive-index detector and two mStyragel HR columns (7.8 mm × 300 mm) linked in series, thermostatted at 60 °C. *N, N*-dimethylformamide containing 0.5 mg/mL LiBr was used as the eluent with a flow rate of 1.0 mL/min. Twelve polystyrene samples of narrow molecular weight distribution were used to calibrate the apparatus. Absorbances at 540 and 570 nm were measured using a Biotek Synergy HT plate reader (Vermont, USA). UV–visible spectra were recorded using a spectrophotometer UV-1280 (Shimadzu) in quartz cuvettes with 10 mm length of the optical pathway. The UV light source consisted of OSRAM Ultravitalux 300 W, set at 20 cm (2 mW / cm^2) from the sample. The visible light source was a Schott KL1500 LCD set at 1 cm from the sample.

2.3. Synthesis of the monomers

Ethyl 4-(4-hydroxyphenyl)azobenzoate (1) [62]. A solution of $NaNO_2$ (4.8 g, 56.4 mmol) in water (30 mL) was added dropwise to a stirred suspension of ethyl 4-aminobenzoate (9.3 g, 56.2 mmol) in HCl 2 M (100 mL) previously cooled around 0–5 °C. Afterwards, phenol (6.34 g, 67.3 mmol) was added. The reaction mixture was kept cooled and stirred for 90 min. Then the reaction mixture was neutralized with a saturated solution of $NaHCO_3$ and filtered. Finally, the solid was recrystallized in methanol: water (1:1), obtaining **1** as a brownish crystalline solid. Yield: 9.4 g (63%), m. p. 162–164 °C; IR: ν_{max} 3389 (OH), 1691 (CO), 1591 cm^{-1} (Ar); NMR data (300 MHz, $CDCl_3$): ^1H, δ 8.17 (d, 2H, H-b), 7.95–7.85 (2d, 4H, H-c, H-f), 6.97 (d, 2H, H-g), 5.95 (bs, 1H, OH), 4.42 (q, 2H, CH_2), 1.43 (t, 3H, CH_3).

Ethyl 4-(4-propynyloxyphenyl)azobenzoate (2) [33]. To a stirred suspension of **1** (16 g, 59.2 mmol) and K_2CO_3 (24 g, 173.6 mmol) in dry acetonitrile (572 mL), propargyl bromide (240 mmol, 26 mL) was added dropwise and the reaction mixture was refluxed for 24 h. Then the reaction mixture was filtered and the solid was recrystallized in ethanol, obtaining an orange crystalline solid. Yield: 14.2 g (78%), m. p. 108–110 °C; IR: ν_{max} 3252 (HC≡), 2126 (C≡C), 1702 (CO), 1599 cm^{-1} (Ar); NMR data (300 MHz, $CDCl_3$): 1H, δ 8.17 (m, 2H, H-b), 7.95 (m, 2H, H-f), 7.90 (m, 2H, H-c), 7.01 (m, 2H, H-g), 4.77 (d, 2H, J 2.0 Hz, H-i), 4.40 (q, 2H, J 7.12 Hz, CH_2CH_3), 2.57 (t, 1H, ≡CH), 1.42 (t, 3H, CH_3); ^{13}C, δ 166.12 (CO), 160.40 (C-h), 155.21 (C-d), 147.49 (C-e), 131.70 (C-a), 130.55 (C-b), 125.08 (C-f), 122.40 (C-c), 115.24 (C-g), 77.92 (C≡C–C), 76.14 (≡CH), 61.21 (CH_2CH_3), 56.04 (C-i), 14.36 (CH_3).

4-(4-propynyloxyphenyl)azobenzoic acid (3) [33]. A suspension of **2** (1 g, 3.24 mmol) in 49 mL of ethanol was refluxed for 10 min. Afterwards, a solution of KOH (0.292 g, 5.2 mmol) in 25 mL of water was added, and the reaction mixture was heated at 85 °C for 2 h. The suspension was filtered and HCl 2 M was added to the resulting solution until pH 3–4. The formed precipitate was filtered and dried, obtaining an orange solid. Yield: 815 mg (90%). NMR data (300 MHz, DMSO–d_6): ^{1}H, δ 8.13 (d, 2H, H-b), 7.98–7.85 (2d, 4H, H-c, H-f), 7.21 (d, 2H, H-g), 4.95 (d, 2H, H-i), 3.65 (t, 1H, ≡C*H*); ^{13}C, δ 167.23 (CO), 160.86 (C-h), 154.84 (C-d), 147.09 (C-e), 132.77 (C-a), 131.06 (C-b), 125.32 (C-f), 122.75 (C-c), 116.06 (C-g), 79.23 (C≡*C*–C), 79.18 (≡*C*H), 56.38 (C-i).

Succinimide 4-(4-propynyloxyphenyl)azobenzoate (4) [63]. To a mixture of **3** (1 g, 3.56 mmol) and *N*-hydroxysuccinimide (0.410 g, 3.56 mmol) in dry acetonitrile (15 mL) and dimethylformamide (5 mL), EDC•HCl (0.85 g, 4.44 mmol) was added. The mixture was stirred under argon atmosphere for 24 h. Afterwards, the reaction mixture was dropped in water, and the resulting precipitate was filtered and dried to obtain an orange solid. Yield: 1.2 g (87%), IR: ν_{max} 3271 (HC≡), 2134 (C≡C), 1765, 1729 (CO), 1597 cm^{-1} (Ar); NMR data (300 MHz, $CDCl_3$): ^{1}H, δ 8.28 (d, 2H, H-b), 8.00–7.90 (2d, 4H, H-c, H-f), 7.12 (d, 2H, H-g), 4.80 (d, 2H, H-i), 2.93 (s, 4H, succ), 2.58 (t, 1H, ≡C*H*).

2-(2-methoxyethoxy)ethyl methanesulfonate (5) [64]. To a stirred mixture of diethylene glycol methyl ether (2 g, 16.65 mmol), triethylamine (2.53 g, 25 mmol) and dry dichloromethane (40 mL) under argon atmosphere at 0 °C, mesyl chloride (1.5 mL, 18.7 mmol) was added dropwise. After 1.5 h, the reaction mixture was washed with water (10 mL), HCl 2 N (5 mL), saturated $NaHCO_3$ solution until basic pH, and water. Organic phase was dried with Na_2SO_4 and concentrated. The residue was purified by column chromatography (ethyl acetate) obtaining a colourless syrup. Yield: 2.9 g (87%). NMR data (300 MHz, $CDCl_3$): ^{1}H, δ 4.38 (m, 2H, MsOCH_2CH$_2$), 3.77 (m, 2H, MsOCH$_2$CH_2), 3.66 (m, 2H, CH$_2$CH_2OCH$_3$), 3.55 (m, 2H, CH_2CH$_2$OCH$_3$), 3.38 (s, 3H, CH$_3$), 3.07 (s, 3H, Ms); ^{13}C, δ 71.83 (*C*H$_2$CH$_2$OCH$_3$), 70.61 (CH$_2$*C*H$_2$OCH$_3$), 69.18 (MsO*C*H$_2$C), 69.05 (MsOCH$_2$*C*), 58.98 (CH$_3$), 37.66 (Ms).

1,12-Diazido-4,9-dioxadodecan-2,11-diol (6) [65]. A mixture of 1,4-butanediol diglycidyl ether (3.3 g, 16.0 mmol), tetrabutylammonium sulfate (0.68 g, 2.0 mmol), and sodium azide (13 g, 200 mmol) in water-dioxane (1:1, 200 mL) was refluxed for 4 h. Then, the reaction mixture was concentrated to about half its volume and extracted with ethyl acetate (3 × 100 mL). The combined organic phase was dried with anhydrous sodium sulfate, filtered, and concentrated to dryness under reduced pressure to obtain a syrupy residue which was purified by column chromatography (*tert*–butyl methyl ether:hexane, 1:1), giving after evaporation of the solvents **6** as a solid (3.2 g, 68%), m.p. 56–58 °C, IR: ν_{max} 3400 (OH), 2087 cm^{-1} (N_3); NMR data ($CDCl_3$): ^{1}H, δ 3.99–3.88 (m, 2H, H-2), 3.55–3.30 (m, 12H, H-1, H-3, H-4), 2.72 (d, 2H, OH), 1.69–1.63 (m, 4H, H-5); ^{13}C, δ 71.92, 71.30 (C-3, C-4), 69.65 (C-2), 53.41 (C-1), 26.27 (C-5).

Diazide monomer 7. To a mixture of **6** (2.4 g, 8.32 mmol), powdered KOH (2.3 g, 41 mmol), tetrabutylammonium bromide (1.07 g, 3.32 mmol) and water (1 mL), a solution of **5** (4.0 g, 20.18 mmol) in toluene (10 mL) was added. The reaction mixture was refluxed for 24 h. Afterwards dichloromethane was added, and the resulting solution was filtered and concentrated. The residue was purified by column chromatography (hexane: acetone 3:1), obtaining a colourless syrup. Yield: 2.3 g (56%), IR: ν_{max} 2094 (N_3), 1106 cm^{-1} (C–O); NMR data (300 MHz, $CDCl_3$): ^{1}H, δ 3.85–3.72 (m, 4H, H-6), 3.69–3.64 (m, 10H, H-2,7,8), 3.68–3.44 (m, 12H, H-3,4,9), 3.40 (s, 6H, H-10), 3.39–3.33 (m, 4H, H-1), 1.6 (m, 4H, H-5); ^{13}C, δ 78.49 (C-2), 71.94 (C-9), 71.33 (C-4), 70.80 (C-7), 70.57 (C-8), 70.12 (C-3), 69.86 (C-6), 59.03 (C-10), 51.94 (C-1), 26.29 (C-5). Anal. Calcd for $C_{20}H_{40}N_6O_8$: C, 48.77; H, 8.19; N, 17.06. Found: C, 48.67; H, 8.351; N, 16.96. HRMS: *m/z* 515.2796 (calcd. for [M]$^+$: 515.2800).

1,12-Diamino-4,9-dioxadodecan-2,11-diol (8). Compound **6** (0.577 g, 2 mmol), Pd/C 10% (0.286 g) and methanol (50 mL) were added to a hydrogenation flask. Hydrogenation was carried out at 40 psi for 3 h. Then, the mixture was filtered through a celite pad, and the solvent evaporated until dryness, obtaining a waxy purple solid. Yield: 0.43 g (90%). NMR data (300 MHz, DMSO–d_6): ^{1}H, δ 3.53–3.40 (m, 2H, H-2′), 3.40–3.30 (m, 4H, H-4′), 3.30–3.24 (m, 4H, H-3′), 2.57 (dd, 2H, $J_{1'a,1'b}$ 12.8 Hz, $J_{1'a,2'}$ 4.4 Hz, H-1′a), 2.41 (dd, 2H, $J_{1'b,2'}$ 6.7 Hz, H-1′b), 1.51 (m, 4H, H-5′); ^{13}C, δ 73.48 (C-3′), 71.37 (C-2′), 70.75 (C-4′), 45.63 (C-1′), 26.45 (C-5′). HRMS: *m/z* 237.1809 (calcd. for [M]$^+$: 237.1809).

2,11-bis(2-(2-methoxyethoxy)ethoxy)−4,9-dioxadodecan-1,12-diamine (9). Compound **7** (0.575 g, 1.17 mmol), Pd/C 10% (0.173 g) and methanol (30 mL) were added to a hydrogenation flask. Hydrogenation was carried out at 40 psi for 3 h. Then, the mixture was filtered through a celite pad, and the solvent evaporated until dryness, obtaining a colourless syrup. Yield: 0.460 g (89%). NMR data (300 MHz, $CDCl_3$): ^{1}H, δ 3.89–3.67 (m, 4H, H-6′), 3.67–3.59 (m, 8H, H-7′,8′), 3.59–3.50 (m, 4H, H-9′), 3.50–3.37 (m, 10H, H-2′,3′,4′), 3.38 (s, 6H, H-10′), 2.90–2.63 (m, 4H, H-1′), 1.68 (bs, 4H, NH), 1.61 (m, 4H, H-5′); ^{13}C, δ 80.67 (C-2′), 71.95 (C-9′), 71.38, 71.30, 70.87, 70.47 (C-3′, 4′, 7′, 8′), 69.52 (C-6′), 59.03 (C-10′), 43.45 (C-1′), 26.37 (C-5′). HRMS: *m/z* 441.3161 (calcd. for [M]$^+$: 441.3170).

Dialkyne monomer 10. To a solution of **4** (0.2 g, 0.53 mmol) in dry dimethylformamide (1 mL) under argon atmosphere, 3,6-dioxaoctan-1,8-diamine (40 μL, 0.266 mmol,) and triethylamine (111 μL, 0.8 mmol) were added. The resulting mixture was stirred for 24 h. Then water was added, precipitate was filtered and purified by column chromatography (dichloromethane-methanol 20:1 to 1:1), obtaining an orange solid. Yield: 0.152 g (85%), m. p. 193–196 °C, IR: ν_{max} 3297 (HC≡, NH), 3064 (Ar), 2134 (C≡C), 1625 (CO), 1596 cm^{-1} (Ar); NMR data (300 MHz, DMSO–d_6): ^{1}H, δ 8.72 (t, 2H, NH), 8.07 (d, 2H, H-b), 7.96 (d, 2H, H-c), 7.92 (d, 2H, H-f), 7.23 (d, 2H, H-g), 4.98 (d, 4H, J 2.3 Hz, H-i), 3.69 (t, 2H, ≡C*H*), 3.66–3.56 (m, 8H, H-2′, 3′), 3.56–3.44 (m, 4H, H-1′); ^{13}C, δ 166.08 (CO), 160.69 (C-h), 153.82 (C-d), 147.08 (C-e), 136.47 (C-a), 128.91 (C-b), 125.18 (C-f), 122.55 (C-c), 116.01 (C-g), 79.21 (*C*≡C), 70.10 (C-3′), 69.34 (C-2′), 56.37 (C-i), 39.8 (C-1′). Anal. Calcd for $C_{38}H_{36}N_6O_6.H_2O$: C, 66.08; H, 5.55; N, 12.17. Found: C, 65.81; H, 5.55; N, 12.11.

Dialkyne monomer 11. To a solution of **4** (0.438 g, 1.16 mmol) in dry dimethylformamide (2.2 mL) under argon atmosphere, **8** (0.137 g, 0.58 mmol) and triethylamine (0.24 mL, 1.75 mmol) were added. The mixture was stirred for 24 h. Then water was added, precipitate was filtered and dried to obtain an orange solid. Yield: 0.34 g (76%), m. p. 172–177 °C, IR: ν_{max} 3292 (HC≡, OH), 2124 (C≡C), 1625 (CO), 1600 cm^{-1} (Ar); NMR data (300 MHz, DMSO–d_6): ^{1}H, δ 8.56 (t, 2H, NH), 8.05 (d, 2H, H-b), 7.94 (d, 2H, H-c), 7.90 (m, 2H, H-f), 7.20 (d, 2H, H-g), 4.97 (d, 2H, J 5.2 Hz, OH), 4.94 (d, 4H, J 2.3 Hz, H-i), 3.82 (m, 2H, H-2′), 3.65 (t, 2H, ≡C*H*), 3.51–3.16 (m, 12H, H-1′, 3′,4′), 1.56 (m, 4H, H-5′); ^{13}C, δ 166.22 (CO), 160.70 (C-h), 153.82 (C-d), 147.11 (C-e), 136.67 (C-a), 128.98 (C-b), 125.19 (C-f), 122.51 (C-c), 116.04 (C-g), 79.23 (*C*≡C), 73.71 (C-3′), 70.89 (C-4′), 68.79 (C-2′), 56.38 (C-i), 43.92 (C-1′), 26.47 (C-5′). Anal. Calcd for $C_{42}H_{44}N_6O_8$: C, 66.30; H, 5.83; N, 11.05. Found: C, 66.04; H, 6.174; N, 11.03.

Dialkyne monomer 12. To a solution of **4** (0.168 g, 0.444 mmol) in dry dimethylformamide (0.84 mL) under argon atmosphere, **9** (0.098 g, 0.222 mmol) and triethylamine (0.1 mL, 0.64 mmol) were added. The mixture was stirred for 24 h. Then water was added, the precipitate was decanted and dried to obtain an orangish syrup. Yield: 0.19 g (89%). NMR data (300 MHz, $CDCl_3$): ^{1}H, δ 8.07–7.85 (m, 6H, H-b,c,f), 7.31 (t, 2H, NH), 7.10 (d, 2H, H-g),

Table 1
GPC[a] data of poly(azoamide triazole)s.

Polymer	Yield (%)	M_w	M_w/M_n
PAAT1	99	148,500	1.24
PAAT2	93	138,000	1.31
PAAT3	85	131,000	1.27
PAAT4	84	95,000	1.46

[a] Determined by GPC analysis with polystyrene standards. Measured in DMF-LiBr.

Table 2
Thermal analysis data of poly(azoamide triazole)s.

Polymer	T_g[a] (°C)	$T_{10\%}$[b] (°C)	T_{dec}[b] (°C)
PAAT1	35.5	318.3	319.5, 382.6
PAAT2	87.7	325.2	304.8, 371.3
PAAT3	2.1	323.6	322.9, 385.0
PAAT4	2.4	325.4	325.8, 390.8

[a] Determined by DSC, second heating.
[b] Measured by TGA.

Table 3
Qualitative solubilities of poly(azoamide triazole)s.

Solvent	PAAT1	PAAT2	PAAT3	PAAT4
TBME	–	–	–	–
Hexane	–	–	–	–
Ethyl acetate	-	–	–	±
Methanol	-	–	–	±
Acetone	–	–	–	++
Chloroform	++	–	–	++
Water	–	–	–	–
DMF	++	±	+	++
DMSO	++	±	++	++

(-) insoluble, (±) slightly soluble, (+) soluble on warming, (++) soluble at room temperature.

4.78 (d, 4H, J 2.4 Hz, H-i), 3.97–3.30 (m, 30H, H-1′–4′, H-6′–9′), 3.27 (s, 6H, H-10′), 2.57 (t, 2H, ≡C*H*), 1.66 (m, 4H, H-5′); ^{13}C, δ 166.96 (CO), 160.26 (C-h), 154.25 (C-d), 147.49 (C-e), 136.07 (C-a), 128.16 (C-b), 124.96 (C-f), 122.55 (C-c), 115.23 (C-g), 77.94 (C–*C*≡C), 77.78 (C-2′), 76.08 (≡*C*H), 71.90, 71.81, 71.45, 70.79, 70.35, 69.6 (C-3′,4′,9′,8′,7′,6′), 58.90 (C-10′), 56,05 (C-i), 41.56 (C-1′), 26.38 (C-5′). Anal. Calcd for $C_{52}H_{64}N_6O_{12}$: C, 64.71; H, 6.68; N, 8.71. Found: C, 62.60; H, 7.06; N, 8.49. HRMS: *m/z* 987.4467 (calcd. for $[M+Na]^+$: 987.4474).

2.4. Synthesis of the polymers

2.4.1. General procedure for the synthesis of poly(azoamide triazole)s (PAATn)

Stoichiometric amounts of diazide and dialkyne were mixed and dissolved in dimethyl sulfoxide. Water was added until a slight cloudiness appeared. Afterwards $CuSO_4$ pentahydrate (20%) and sodium ascorbate (40%) were added, and the reaction mixture was stirred and heated to 50 °C under argon atmosphere for 24 h. Reaction mixture was then processed in different ways depending on the polymer formed. Polymer **PAAT1** was recovered by precipitation in *tert*–butyl methyl ether (TBME), followed by re-dissolution in dichloromethane and precipitation in acetone. Polymers **PAAT2** and **PAAT3** were isolated by filtration on a glass filter and washed with water and acetone. These polymers were purified by dissolution in dimethyl sulfoxide and precipitation in TBME. Polymer **PAAT4** was also isolated by filtration but purified by dissolution in CH_2Cl_2 and precipitation in TBME. Tables 1–4 show the studied characteristics of the prepared polymers. The infrared and NMR spectroscopy data are listed below.

Table 4
UV Absorption data of the **PAATn** polymers in DMSO.

Compound	λ (nm)
10	429, 357, 255
11	437, 358, 255
12	449, 357, 255
PAAT1	426, 360, 255
PAAT2	432, 359, 255
PAAT3	432, 360, 255
PAAT4	442, 361, 256

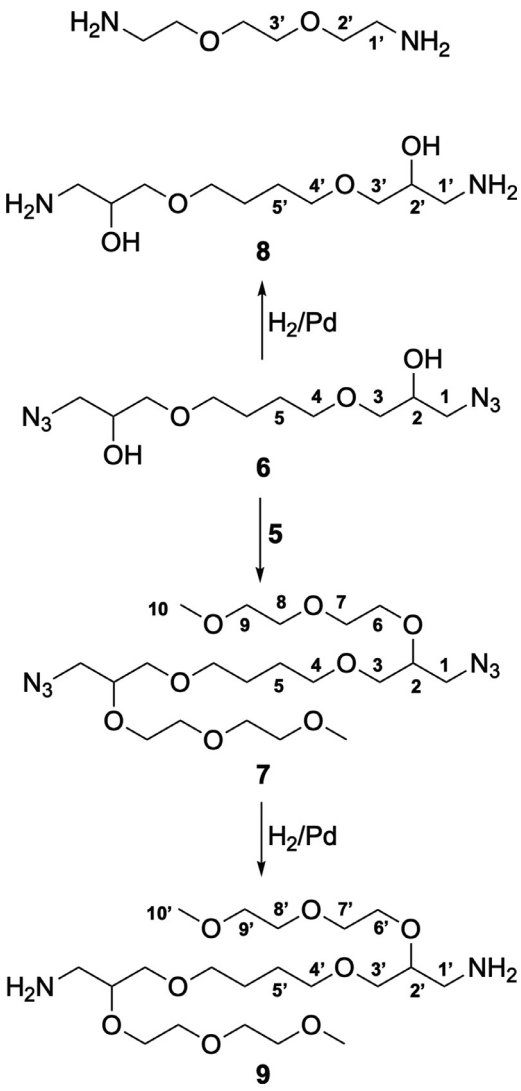

Fig. 1. Synthesis of diazides and diamines.

PAAT1. IR: ν_{max} 3326 (NH), 1644 cm^{-1} (CO); NMR data (500 MHz, $CDCl_3$): ^{1}H, δ 7.95 (s, 2H, H-j), 8.00–7.80 (m, 12H, H-b,c,f), 7.10 (d, 4H, H-g), 6.90 (bs, 2H, NH), 5.30 (s, 4H, H-i), 4.64 (bd, 2H, H-1a), 4.42 (dd, 2H, $J_{1b,2}$ 6.94 Hz, $J_{1a,1b}$ 14.0 Hz, H-1b), 3.86 (bs, 2H, H-2), 3.80–3.30 (m, 36H, H-1′,2′,3′,3,4,6,7,8,9), 3.30 (s, 6H, H-10), 1.63 (bs, 4H, H-5); ^{13}C, δ 166.96 (CO), 161.19 (C-h), 154.37 (C-d), 147.20 (C-e), 143.18(C-k), 135.67 (C-a), 127.98 (C-b), 125.08 (C-f), 124.90 (C-j), 122.63 (C-c), 115.16(C-g), 77.73 (C-2), 71.87, 71.43, 70.65, 70.41, 70.31, 69.84, 69.68 (C-2′,3′,3,4,6,7,8,9), 62.21 (C-i), 58.95 (C-10), 51.62 (C-1), 39.88 (C-1′), 26.30 (C-5).

PAAT2. IR: ν_{max} 3309 (OH, NH), 1630 cm^{-1} (CO); NMR data (500 MHz, DMSO–d_6): ^{1}H, δ 8.67 (bs, 2H, NH), 8.19 (s, 2H, H-j),

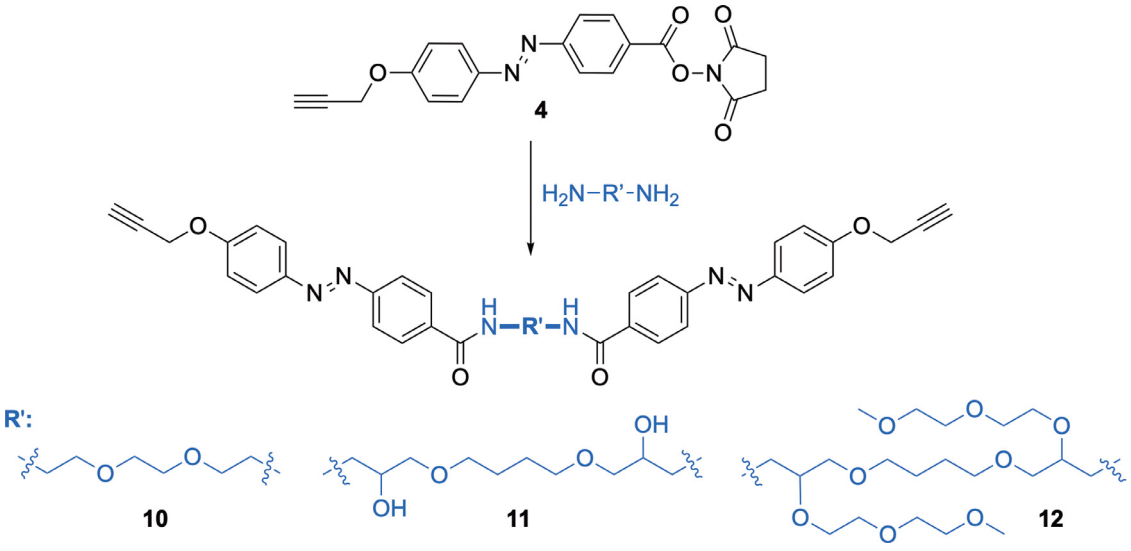

Fig. 2. Synthesis of dialkyne monomers.

8.02 (d, 4H, H-b), 7.91, 7.87 (2d, 8H, H-c,f), 7.25 (d, 4H, H-g), 5.32 (d, J 5.1 Hz, OH), 5.26 (s, 4H, H-i), 4.48 (bd, 2H, H-1a), 4.31 (dd, 2H, $J_{1b,2}$ 7.8 Hz, $J_{1a,1b}$ 13.6 Hz, H-1b), 3.99 (bs, 2H, H-2), 3.62–3.20 (m, 20H, H-1′,2′,3′,3,4), 1.56 (bs, 4H, H-5); ^{13}C, δ 166.11 (CO), 161.65 (C-h), 153.83 (C-d), 146.80 (C-e), 142.27(C-k), 136.37 (C-a), 128.89 (C-b), 126.21 (C-j), 125.29 (C-f), 122.51 (C-c), 115.87 (C-g), 72.54, 70.94, 70.07, 69.31, 68.71 (C-2′,3′,3,4,2), 61.97 (C-i), 53.43 (C-1), 40.84 (C-1′), 26.32 (C-5).

PAAT3. IR: ν_{max} 3399 (OH, NH), 1644 cm^{-1} (CO); NMR data (500 MHz, DMSO–d_6): ^{1}H, δ 8.54 (bs, 2H, NH), 8.23 (s, 2H, H-j), 8.04 (bd, 4H, H-b), 7.92, 7.89 (2bd, 8H, H-c,f), 7.25 (d, 4H, H-g), 5.28 (s, 4H, H-i), 4.96 (bs, 2H, OH), 4.58 (m, 2H, H-1a), 4.43 (m, 2H, H-1b), 3.84 (m, 4H, H-2′,2), 3.60–3.10 (m, 36H, H-1′,3′,4′,3,4,6,7,8,9), 3.18 (s, 6H, H-10), 1.55 (bs, 8H, H-5′,5); ^{13}C, δ 166.23 (CO), 161.60 (C-h), 154.84 (C-d), 146.84 (C-e), 142.48(C-k), 136.58 (C-a), 128.97 (C-b), 126.21 (C-j), 125.27 (C-f), 122.46 (C-c), 115.93 (C-g), 77.39 (C-2), 73.71, 71.68, 70.93, 70.67, 70.30, 69.95, 69.26, 68.81 (C-2′,3′,4′,3,4,6,7,8,9), 61.99 (C-i), 58.47 (C-10), 51.09 (C-1), 43.92 (C-1′), 26.47, 26.32 (C-5′,5).

PAAT4. IR: ν_{max} 3336 (NH), 1644 cm^{-1} (CO); NMR data (500 MHz, $CDCl_3$): ^{1}H, δ 8.05–7.85 (m, 14H, H-j,b,c,f), 7.30 (bs, 2H, NH), 7.14 (d, 4H, H-g), 5.31 (s, 4H, H-i), 4.68 (m, 2H, $J_{1a,2}$ 2.9 Hz, H-1a), 4.44 (m, 2H, $J_{1b,2}$ 7.3 Hz, $J_{1a,1b}$ 14.3 Hz, H-1b), 4.00–3.15 (m, 56H, H-1′,2′,3′,4′,2,3,4,6′,6,7′,7,8′,8,9′,9), 3.33, 3.28 (2 s, 12H, H-10′,10), 1.67 (m, 8H, H-5′,5); ^{13}C, δ 166.97 (CO), 161.15 (C-h), 154.29 (C-d), 147.25 (C-e), 143.19 (C-k), 136.02 (C-a), 128.12 (C-b), 125.01 (C-f), 124.83 (C-j), 122.52 (C-c), 115.16 (C-g), 77.81, 77.75 (C-2′,2), 71.86, 71.79, 71.43, 70.77, 70.65, 70.40, 70.33, 69.68, 69.59 (C-3′,3,4′,4,6′,6,7′,7,8′,8,9′,9), 62,23 (C-i), 58.93, 58.86 (C-10′,10), 51.64 (C-1), 41.57(C-1′), 26.36, 26.29 (C-5′,5).

2.5. Alternating irradiation of the sample with ultraviolet and visible light

A solution of the polymer (0.028 mg/mL) in dimethyl sulfoxide was consecutively irradiated with ultraviolet light, for different periods of time, followed by visible light for 1 min. The solution was studied by ultraviolet-visible spectroscopy after each irradiation.

2.6. Degradation of polymers

2.6.1. Degradation in buffer solution

The hydrolytic degradation study was carried out on films prepared by evaporations of polymer solutions **PAAT1** and **PAAT4** in dichloromethane (20 mg/mL). Films formed were dried under vacuum until no weight loss was observed. The thickness of the films obtained was approximately 70 μm. Afterwards, 10 mL of buffered solutions at different pH were added, and they were incubated at either 37 or 70 °C. After different periods of time, about 40 days, the sample was recovered by filtration, and the film was washed with distilled water and dried under vacuum. Finally, the remaining film was analyzed by Gel Permeation Chromatography.

2.6.2. Degradation with dithionite

*2.6.2.1. Degradation of monomer **12**.* To a solution of **12** in methanol (5 mg, 1.5 mL) water was added until turbidity (0.7 mL). Then, sodium dithionite (10 equivalents) was added and stirred at 37 °C protected from light. The reaction mixture was monitored by TLC, adding more dithionite until reduction was complete. After four days, the solvent was evaporated to dryness and dichloromethane was added to obtain a suspension. The solid formed was filtered off and the filtrate was evaporated again *in vacuo*. Finally, the mixture obtained was dried to constant weight, being used directly for its analysis by UV-visible spectroscopy, in order to evaluate the reduction of the azo group.

2.6.2.2. Degradation of polymer. Polymers **PAAT1** and **PAAT4** were dissolved in CH_2Cl_2 (4 mg/mL), and the solvent was slowly removed by evaporation at room temperature to obtain a film that was dried under vacuum to constant weight. Afterwards, a pH 6 buffered solution of sodium dithionite (155 mM, 2.0 mL) was added, and the vials were heated at 37 °C with stirring. Samples were withdrawn at 2, 4, 8 and 11 days, replacing the sodium dithionite solution in the remaining samples. The film was washed with distilled water and dried. Finally, the samples were analyzed by size exclusion chromatography.

2.7. Biocompatibility studies

2.7.1. Sample preparation

Polymers **PAAT1** and **PAAT4** were dissolved in DMSO for cell culture (4 mg/mL). Then, 200 μL of each solution was added to a 96-well plate, and DMSO was removed in a vacuum oven until dryness, obtaining the wells coated with thin films of the samples to be analyzed.

2.7.2. Hemolysis assay

Toxicity to human red blood cells (hRBC) was tested by carefully preparing a mixture of fresh human blood and PBS. The mixture

was centrifuged at 700 G for 10 min, supernatant was discarded, and the procedure was repeated three times. Then, PBS was added to prepare a 5% (v/v) suspension of hRBC. Aliquots of this suspension (150 µL) was added to each coated well. PBS (150 µL) was used as blank and hRBC suspension (150 µL) containing 1% of Triton X-100 was used as positive control (total hemolysis). The 96-wells plate was incubated for 1 hour at 37 °C. Then, centrifuged for 10 min at 700 G. Supernatants were placed in a new microtiter plate and absorbance was measured at 540 nm. The experiment was performed three times in triplicate, and the equation to calculate the hemolytic activity is:

$$\%\ hemolysis = \left[\left(A_{540}^{polymer} - A_{540}^{negative} / A_{540}^{positive} - A_{540}^{negative}\right)\right] x\ 100$$

2.7.3. Cell culture

DMEM was supplemented with 10% of FBS, 1% Penicillin and streptomycin, 1% L-glutamine, 1% sodium pyruvate and 1% non-essential aminoacids. A cryotube containing 0.5 million of Human Gingival Fibroblasts (HGnF) cells was heated to 37 °C, diluted with 9 mL of DMEM and centrifuged at 300 G for 5 min. Supernatant was discarded and pellet resuspended in 5 mL of supplemented DMEM. Then, plated in a cell culture flask and incubated at 37 °C with 5% CO_2. After 48 h, the medium was removed, the culture was washed with PBS, and treated with trypsin-EDTA. HGnF were counted and diluted with DMEM to obtain a suspension of 1×10^5 cells per milliliter. Then, 150 µL of the cell suspension were added to the wells of a 96-wells plate to seed 1.5 10^4 HGnF per well. 96-wells plate was incubated for 24 h at 37 °C with 5% CO_2.

2.7.4. MTT assay

To evaluate the toxicity produced by **PAAT1** and **PAAT4**, a cell viability test was carried out using the MTT method, which consists of reducing this tetrazolium dye to a water-insoluble crystal (formazan). To perform this assay, a 96 wells microtiter plate was prepared according to the Section 2.7.1. A HGnF suspension (150 µL) containing 1×10^5 cells per milliliter was added to each polymer coated well. HGnF suspension (150 µL) was dispensed to a well which did not contain any polymer as positive control. Wells containing only supplemented DMEM was used as negative control. Microtiter plate was incubated at 37 °C with 5% CO_2. After 24 h, 20 µL of a MTT solution (5 mg/mL) was added to each well and microtiter plate was incubated. After 4 h, supernatant was carefully withdrawn and 150 µL of DMSO was added to dissolve the formazan crystals and films. This solution was transferred to a new microtiter plate and absorbance of the solutions was measured at 570 nm using a microplate reader. This assay was repeated three times in triplicate. Positive control was used as 100% of viability, and results of the samples were relative to this positive control.

3. Results and discussion

3.1. Synthesis and chemical structure of the azo polymers

In this work, we describe the preparation of four novel linear poly(azoamide triazole)s, referred to as **PAATn**, which were prepared from diazide (**6, 7**) and dialkyne functionalized monomers (**10**–**12**) (Figs. 1 and 2, respectively), by CuAAC polyaddition reaction in solution. Diazide monomer **6** was readily prepared from commercially available 1,4-butanediol diglycidyl ether by opening of the epoxide rings with sodium azide as nucleophile [65].

Afterward, the alcohol functions obtained in the opening of the epoxides were reacted with 2-(2-methoxyethoxy)ethyl methanesulfonate (**5**), previously prepared according to a procedure described in the literature [64], to obtain monomer **7**.

The synthesis of dialkyne monomers **10, 11** and **12** were conveniently carried out by reaction of active ester **4**, prepared as displayed in Fig. 3 in four steps by previously described methods [63], with three different diamines: commercial 3,6-dioxaoctan-1,8-diamine and diamines **8** and **9**, respectively (Fig. 1). These diamines were easily obtained in high yield by reduction of the diazide functions of the corresponding monomers **6** and **7** (Fig. 1). All these compounds were conveniently characterized by infrared, ^1H and ^{13}C NMR spectroscopies, elemental analysis and/or high-resolution mass spectrometry.

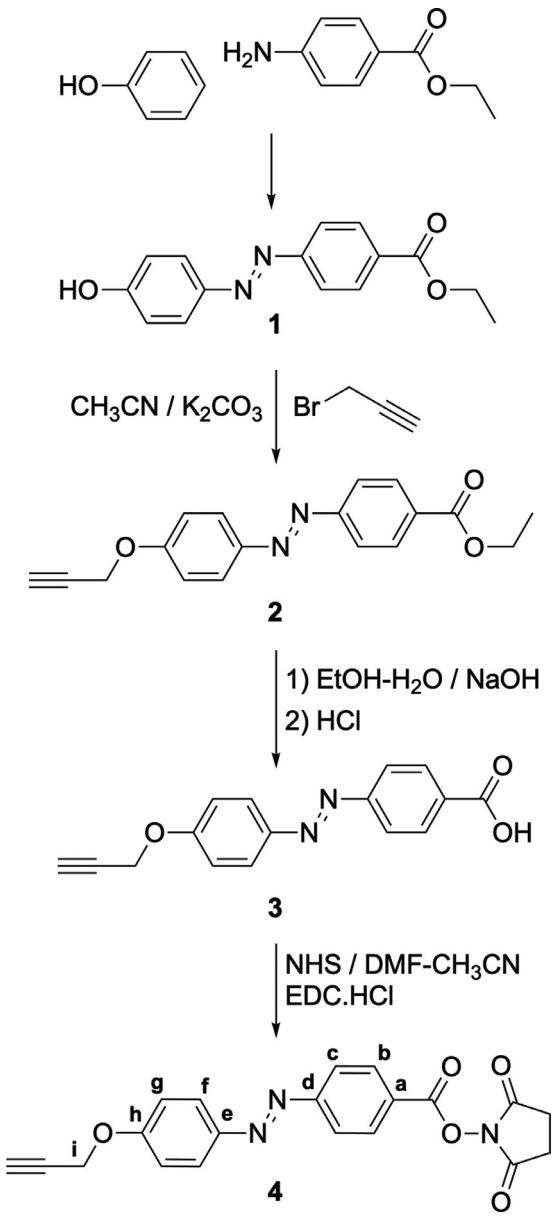

Fig. 3. Synthesis of the azobenzene derivatives.

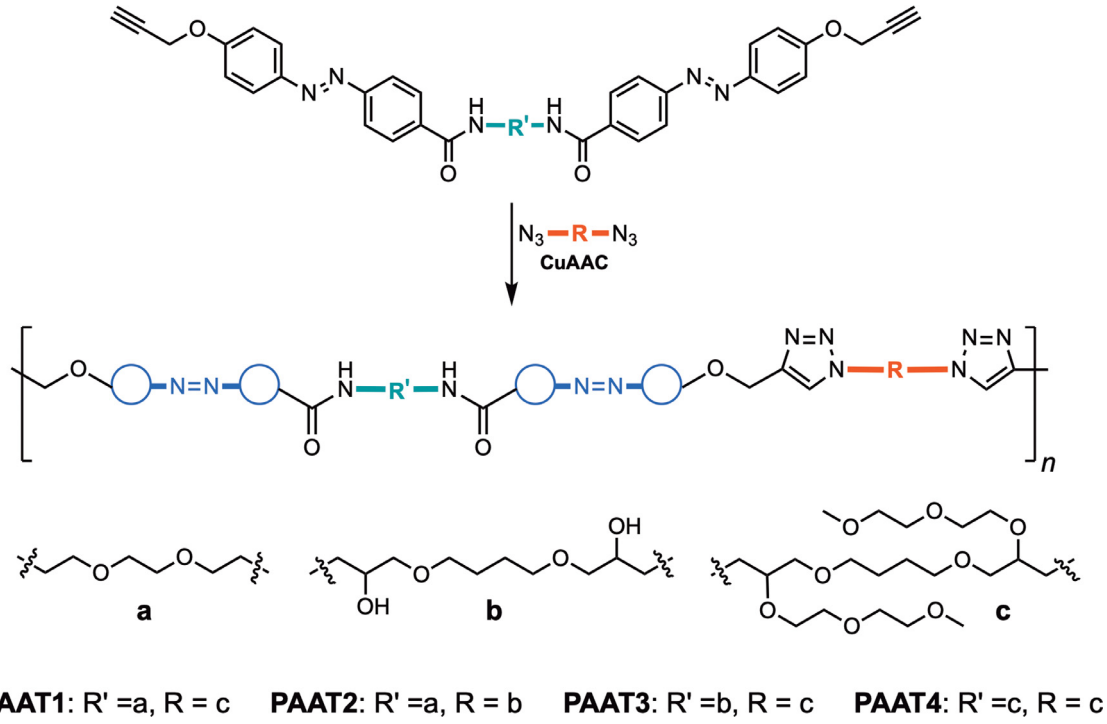

Fig. 4. Synthesis of the **PAATn** polymers.

The azo polymers **PAATn** were prepared by polymerization of the bis-azide and bis-alkyne monomers using copper-catalyzed azide–alkyne cycloaddition (CuAAC) reactions (Fig. 4). These polymers were isolated in yields greater than 80% (Table 1) and were purified as described in the experimental part.

The chemical compositions anticipated for these poly(azoamide triazole)s were confirmed by FTIR and NMR spectroscopy, and the corresponding data are detailed in the experimental section. All the FTIR spectra displayed the expected absorption bands of the amide functions presents along the polymer chain. No residual bands corresponding to azide or alkyne functional groups of the starting monomers were detected in the corresponding polymeric materials. The absorption bands appearing around 3300 and 1650 cm^{-1} were attributed to the stretching band of NH and carbonyl group of the amide functions, respectively.

As an example, the ^{1}H and ^{13}C NMR spectra (Figs. 5 and 6, respectively) of poly(azoamide triazole) **PAAT2**, recorded in deuterated dimethyl sulfoxide, are displayed with the structural correlation of the signals that appear in both types of spectrum. The ^{1}H NMR spectrum of **PAAT2** (Fig. 5) shows five signals in the region of 8.80 to 7 ppm. The signals appearing as singlets at approximately 8.70 and 8.20 ppm were attributed to the amide function present in the bis-alkyne monomer, and to the H-j protons of the 1,4-disubstituted triazole aromatic ring obtained in the CuAAC reaction, respectively. Likewise, the hydroxyl groups present in the repeating unit of this polymer give rise to the signal that appears at 5.30 ppm, as a doublet, displaying a coupling constant of about 5 Hz. The proposed structure for the **PAAT2** polymer is also confirmed by its ^{13}C NMR spectrum (Fig. 6). According to the regioselectivity expected in the CUAAC polymerization reaction, the polymer should have 1,4-disubstituted 1,2,3-triazole rings in its structure. This ring produces two signals in the ^{13}C NMR spectrum at 142.27 and 126.21 ppm that were attributed to the C-K and C-j carbons of the triazole, respectively.

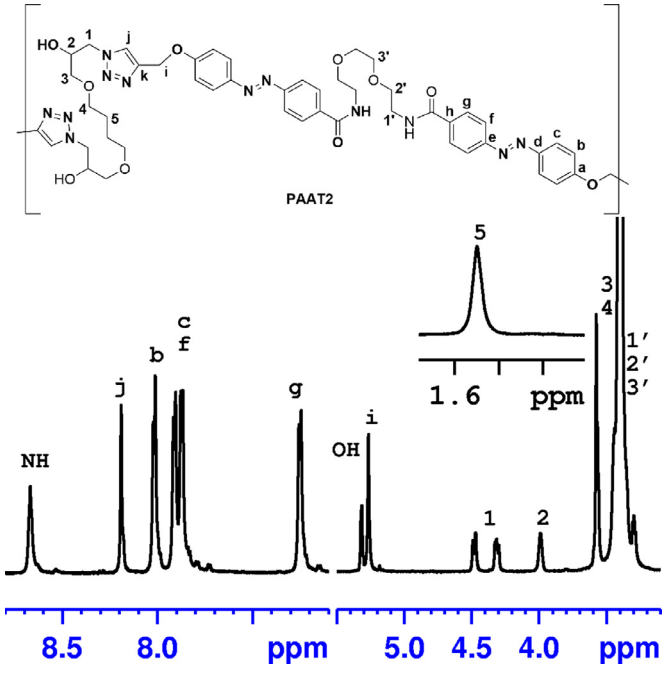

Fig. 5. ^{1}H NMR spectrum of **PAAT2** recorded in deuterated dimethyl sulfoxide.

3.2. Gel permeation chromatography

The purity of all polymers was confirmed by size exclusion chromatography, using μStyragel columns calibrated against polystyrene standards, finding that the chromatograms of the **PAATn** polymers were unimodal. Mass-averaged molar masses (Mw), measured using lithium bromide in dimethylformamide as mobile phase, showed values between 95,000 and 148,000 g/mol (Table 1). The apparent molar masses of the azo homopolymers

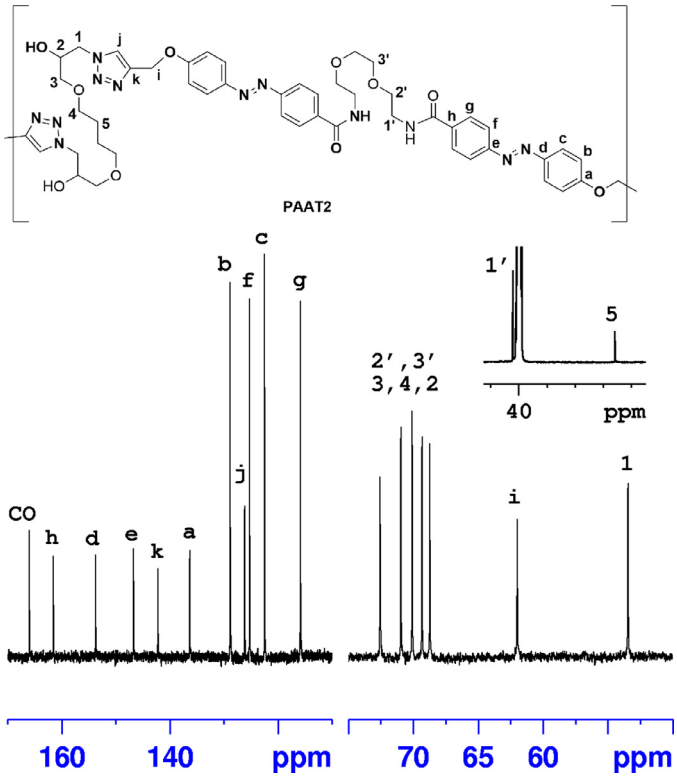

Fig. 6. ^{13}C NMR spectrum of **PAAT2** recorded in dimethyl sulfoxide.

PAAT1, PAAT2 and **PAAT3** are quite like each other while **PAAT4** has a clearly lower molar mass.

However, the **PAATn** polymers have different chemical structures so they are expected to have different hydrodynamic volumes for the same absolute molar mass. This makes it difficult to make comparisons between the apparent molar masses measured by GPC for these polymers.

3.3. Thermal analysis

The thermal study of the poly(azoamide triazole)s **PAATn** was carried out using a combination of DSC and TGA. The data resulting from this study are shown in Table 2. The DSC study revealed that all the polymers exhibited one glass transition step (Tg) during the second heating trace measured with a heating rate of 10 °C/min. Annealing experiments were carried out to favor that the intermolecular interactions could lead to the crystallization of the samples. However, under the tested conditions the thermograms only showed the presence of glass transitions. The **PAAT2** polymer has the highest Tg value (Tg 87.7 °C) while the **PAAT3** and **PAAT4** polymers have much lower values of Tg, about 2 °C. In view of these data (Table 2), it seems that the values of the glass transition could be related to the separation of the azobenzene groups, which are the most rigid segments along the macromolecules main chain. Thus, the **PAAT1** and **PAAT2** polymers, where the azobenzene groups are separated by segments containing 8 atoms, display higher Tg values than the **PAAT3** and **PAAT4** polymers where these segments always contain 12 atoms. Likewise, the presence or absence of diethylene glycol side chains also affects the Tg values. Thus, polymer **PAAT1** have a Tg value lower than **PAAT2** due to the diethylene glycol side chains of monomer **7**, possibly exerting a plasticizing effect.

Thermogravimetric analysis of the **PAATn** polymers was performed by TGA, under inert atmosphere and heating the sample from room temperature to 600 °C. Table 2 shows the values obtained from the thermogravimetric analysis of the polymers. The temperatures at 10% weight loss determined at a heating rate of 10 °C/min were higher than 315 °C (Table 2), which shows its good thermal stability. All polymers thermally decompose in two stages, as it is shown in Table 2. Although the decomposition temperature values are quite similar, it can be observed that the polymers that have free alcohol functions in the main chain, **PAAT2** and **PAAT3**, present somewhat lower decomposition temperature values than their analogues with diethylene glycol side chains, **PAAT1** and **PAAT4**.

3.4. Qualitative solubilities

Table 3 shows the solubilities [66] of **PAATn** polymers in different solvents. None of the synthesized polymers was soluble in water, but they were dissolved in dimethyl sulfoxide or dimethylformamide.

In general, they were also not soluble in common organic solvents. It can be observed that the **PAAT2** and **PAAT3** polymers, which contain free secondary alcohol functions along the polymer chain, have lower solubility than the other polymers in common organic solvents. Thus, for example, **PAAT1** is easily soluble in chloroform or the polymer **PAAT4** can be dissolved in several organic solvents.

3.5. Photophysical properties

Solutions of the **PAATn** polymers in dimethyl sulfoxide, kept in the dark overnight, were used to obtain their ultraviolet-visible spectra. The values corresponding to the maximum absorption are shown in Table 4.

The absorption spectra of azobenzenes are known to consist of three main bands appearing at approximately 430, 320 and 230 nm, and which are assigned to the n-π^*, π-π^* transitions for *trans* azobenzene and π-π^* in the phenyl rings, respectively.

Similar bands appear in the absorption spectra corresponding to the **PAAT1**-**PAAT4** polymers, which in turn are very similar to the spectra exhibited by the respective monomers **10**–**12**, from which they are prepared. The polymers were irradiated with an ultraviolet lamp placed at 20 cm from the sample. Fig. 7 shows how the band that appears at 320–400 nm, corresponding to the absorption of *trans*-azobenzene, progressively decreases as the irradiation time with UV light increases due to its isomerization to *cis*-azobenzene. As can be seen, the **PAAT1** polymer reached the photostationary state after 240 s (Fig. 7A), while the rest of the polymers needed only 180 s to reach the maximum degree of photoisomerization (Fig. 7B-D). The degree of photoisomerization achieved is not high, probably because the azobenzene groups are forming part of the main chain, which will hinder their movements. The reversibility of photoisomerization was studied by ultraviolet–visible spectroscopy employing two different methods: thermally and by irradiating with visible light. Thus, if previously UV irradiated samples are exposed to visible light, the absorption band at 320–400 nm increases markedly until it almost recovers its initial absorbance, which represents the isomerization of *cis*-azobenzene to *trans*-azobenzene. This process of interconversion between the *cis*- and *trans*-azobenzene remains reversible when irradiation cycles with UV and visible light are carried out consecutively for all the polymers. Fig. 8 illustrated the *cis-trans-cis* reversibility process for polymer **PAAT1** as an example.

As previously mentioned, we also studied the reversibility of photoisomerization by a thermal method. Thus, for example, when a **PAAT1** polymer solution in DMSO was irradiated with ultraviolet light, and subsequently kept in the dark at 60 °C, it was possible to verify how the absorbance of the solution (band at about 360 nm) increased with heating time. After 45 min of heating at

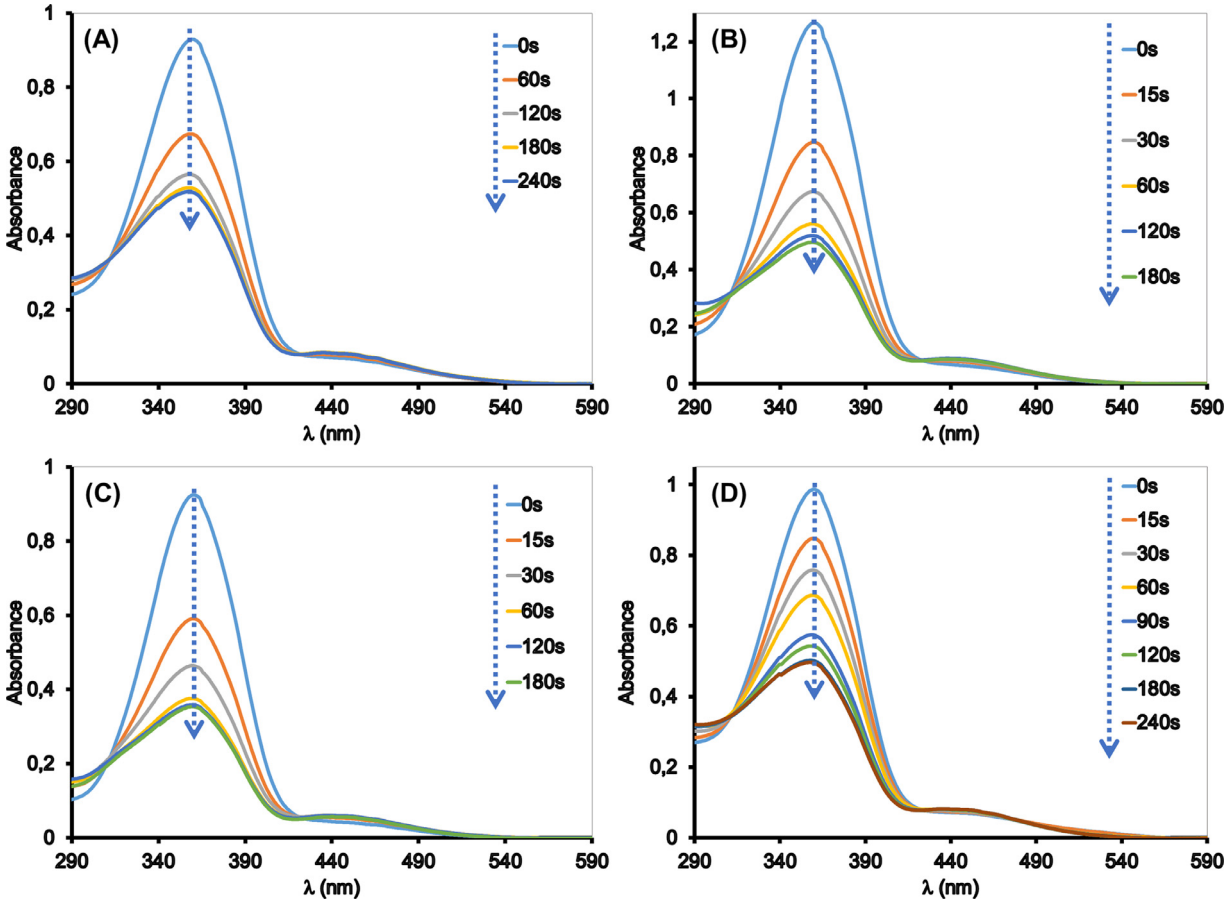

Fig. 7. UV-Visible spectra illustrating the photoisomerization of PAAT1 (A), PAAT2 (B), PAAT3 (C) and PAAT4 (D). All spectra were registered in DMSO.

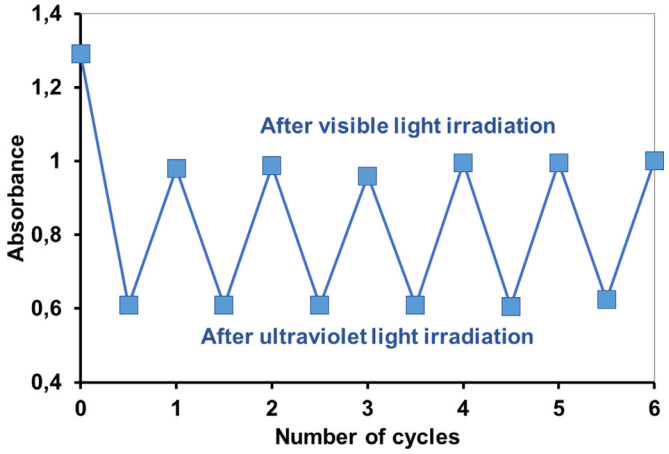

Fig. 8. Reversibility of photoisomerization of **PAAT1** solution for the *trans*-to-*cis* and *cis*-to-*trans* processes. The sample was alternately irradiated with ultraviolet light for 300 s and visible light for 30 s.

60 °C the absorbance reached the initial value. If this same experiment is carried out at room temperature, it would take four days to reach a value close to the initial one.

3.6. Degradation of polymers

The sensitivity of these polymers to hydrolysis has been studied under different conditions. As expected, the amide functions present in the structure of these polymers can hydrolyze under relatively drastic conditions, being stable in a physiological environment. The hydrolysis of **PAATn** polymers has been studied at pH 2.0, 7.4, and 10, and at different temperatures, 37 and 70 °C, for several months.

Likewise, taking advantage of the fact that, in addition to the amide functions, there are also azo functions, a degradation experiment that implied the breaking of this bond and therefore the breaking of the polymer chain was carried out.

All these degradation experiments have been studied by following the variation of the molar masses of the samples subjected to degradation by means of size exclusion chromatography.

3.6.1. Buffered degradation

The results of the hydrolytic degradation studies are shown in Figs. 9 and 10, where the decrease in molar mass of the degraded samples is shown against the degradation time. The hydrolytic degradations of polymers **PAAT1** and **PAAT4** have been studied at 37 °C and in solutions buffered at pH 7.4 and pH 10 for 10 months. It was observed that under these conditions both the number- and mass-average molar masses at the end of study was practically the same as the initial one for **PAAT4** (Fig. 10), or it had slightly decreased at the beginning of the degradation to remain practically constant until the end of the study, as in the case of **PAAT1** (Fig. 9). However, it was found that if instead of carrying out the hydrolytic degradation under physiological conditions, pH 7.4 and temperature 37 °C, it was done at a higher temperature, 70 °C, the degradation of the polymer occurred, as expected, faster. Under these conditions, the **PAAT4** polymer, that did not show degradation under physiological conditions, now did show a continuous decrease in its number- and mass-average molar masses values (Fig. 10).

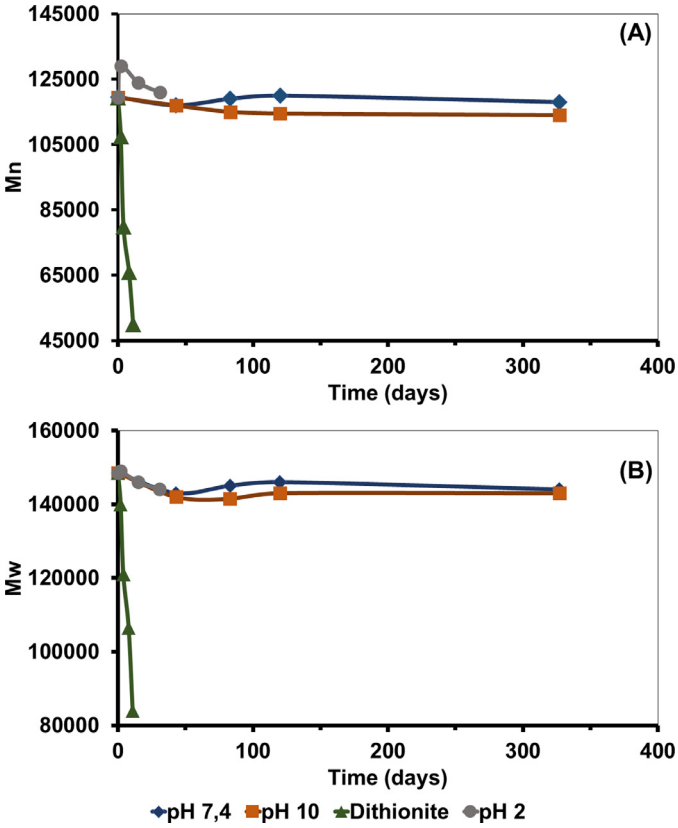

Fig. 9. Hydrolytic degradation of **PAAT1** under different conditions: (A) number-average molar mass *vs* incubation time; (B) mass-average molar mass *vs* incubation time.

Degradation at pH 2 has also been studied for about a month. An increase in molar mass was observed in the first days of degradation and then it slowly decreased. The increase in molar mass is most likely due to the leaching of low molecular weight molecules (Fig. 9).

3.6.2. Dithionite degradation

In this study, the reducing agent used was sodium dithionite, a chemical compound that mimics the enzyme azoreductase and which has previously been used for this same purpose [30,31,35,60,61].

The reduction reaction was first tested with monomer **12**, to evaluate the efficiency of the reductive cleavage of the azo function which was followed by ultraviolet spectroscopy. Thus, upon treatment of a solution of **12** in a mixture of methanol/water at 37 °C with an excess of sodium dithionite for several days, the azo function of the monomer was reduced into their corresponding amines. It was observed that the deep yellow color of the monomer solution disappeared as the reduction reaction progressed. Likewise, ultraviolet-visible spectroscopy demonstrated that during the reaction of the monomer with sodium dithionite the intensity of the absorption band corresponding to the azobenzene group (Fig. 11a) gradually decreased with time (Fig. 11b).

The degradation studies of **PAAT1** and **PAAT4** were carried out by treating polymer films with a buffered solution of sodium dithionite at 37 °C. Size exclusion chromatography was used to follow the degradation process. Figs. 9 and 10 show the evolution of the average molar mass values for the **PAAT1** and **PAAT4** polymers with degradation time upon treatment with $Na_2S_2O_4$. As can be seen, the number- and mass-average molar mass values decreased continuously and rapidly with the incubation time indicating a degradation of the main chain of these polymers (Fig. 12).

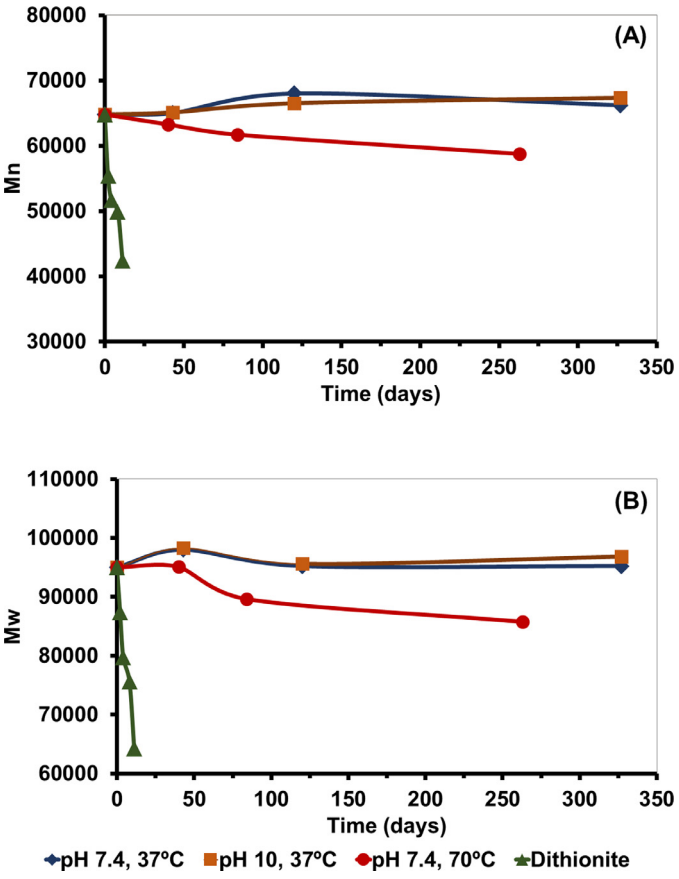

Fig. 10. Hydrolytic degradation of **PAAT4** under different conditions: (A) number-average molar mass *vs* incubation time; (B) mass-average molar mass *vs* incubation time.

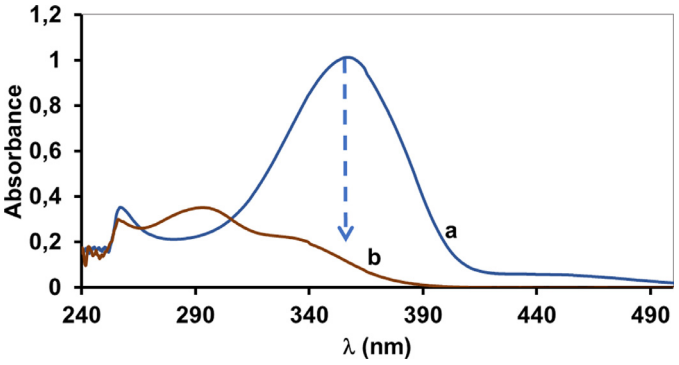

Fig. 11. UV-visible spectra illustrating the degradation of monomer **12** in the presence of sodium dithionite; (a) monomer **12**, (b) after degradation.

Likewise, a slight color change of the films could be observed with the degradation.

3.7. Biocompatibility

Biocompatibility studies were carried out testing the capacity of **PAAT1** and **PAAT4** to produce the lysis of hRBC. Release of hemoglobin was measured by absorbance at 540 nm following previously reported protocols [67] with minor modifications. Percentage of hemolysis was among 0.28% and 1.36%, which appears to be residual hemolysis (Table 5). We have also examined the toxicity that these films produced when HGnF were cultured over the coated wells in a 96-wells plate. After 24 h of incubation, cell viability was measured through reliable and well known MTT method.

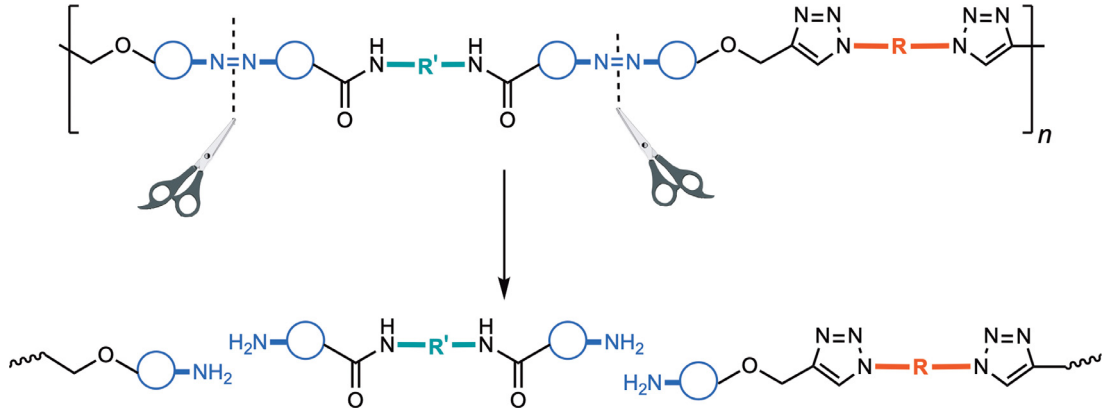

Fig. 12. Dithionite degradation of the main chain of PAATn polymers.

Table 5
Hemolysis and cell viability.

Polymer	% hemolysis[a]	% cell viability[b]
PAAT1	1.07 ± 1.18	229 ± 48
PAAT4	1.36 ± 0.37	181 ± 35

[a] Relative to the positive control of hRBC with surfactant Triton-X 100.
[b] Relative to the positive control of HGnF without polymer.

Absorbance was measured at 570 nm, wavelength at which **PAAT1** and **PAAT4** do not absorb (Fig. 7). We found that the polymer films were not only nontoxic to HGnF, but coated wells also exhibited a higher bioactivity than positive control (Table 5). One of the probable causes that may influenced growth in coated wells is that those films offered to HGnF a nontoxic porous three-dimensional physical shape which allowed a better oxygenation and nutrient accessibility [68].

4. Conclusions

Novel sensitive to reduction poly(azoamide triazole)s were successfully synthesized via the azide-alkyne cycloaddition reaction catalyzed with copper (I) (CuAAC). All the polymers were obtained as amorphous solids, observing that all the polymers were insoluble in water and those polymers that did not contain alcohol functions in their structure were soluble in chloroform or other organic solvents. The sensitivity of synthetized azo polymers to hydrolysis has been studied in different conditions. Thus, there was practically no alteration of the polymer films when they were subjected to degradation under physiological conditions, but a continuous and slow degradation did occur when the temperature was raised to 70 °C. Likewise, a very considerable increase in the degradation of the films was also observed when they were subjected to the treatment with $Na_2S_2O_4$, a reducing compound that simulates the enzyme azoreductase which exists in the colon. Hemolysis and cytotoxicity tests imply that tested polymers could be suitable for biomedical purposes. Therefore, these azo polymers could have utility as coatings for drugs that must be specifically released in the colon.

Declaration of Competing Interest

The authors declare that they have no known competing financial interests or personal relationships that could have appeared to influence the work reported in this paper.

CRediT authorship contribution statement

Adrián Suárez-Cruz: Conceptualization, Investigation, Methodology, Writing – original draft. **Inmaculada Molina-Pinilla:** Conceptualization, Validation, Supervision, Writing – review & editing. **Khalid Hakkou:** Investigation, Methodology, Resources, Writing – original draft. **Cristian Rangel-Núñez:** Conceptualization, Investigation, Methodology, Writing – original draft. **Manuel Bueno-Martínez:** Conceptualization, Funding acquisition, Project administration, Supervision, Writing – original draft.

Acknowledgments

The authors acknowledge the Ministerio de Economía y Competitividad (grant MAT2016-77345-C3-2-P) of Spain and the Universidad de Sevilla (VI Plan Propio, PP2021/00000658) for supporting this work. A.S.C. is grateful for a scholarship granted by VI-PPITUS de la Universidad de Sevilla.

References

[1] P. Xiao, J. Zhang, J. Zhao, M.H. Stenzel, Light-induced release of molecules from polymers, Prog. Polym. Sci. 74 (2017) 1–33, doi:10.1016/j.progpolymsci.2017.06.002.
[2] J. Wang, S. Li, B. Wu, Y. He, Enzyme responsive self-assembled amphiphilic diblock copolymer synthesized by the combination of NMP and macromolecular azo coupling reaction, Eur. Polym. J. 84 (2016) 236–244, doi:10.1016/j.eurpolymj.2016.09.030.
[3] Z.G. Ma, R. Ma, X.L. Xiao, Y.H. Zhang, X.Z. Zhang, N. Hu, J.L. Gao, Y.F. Zheng, D.L. Dong, Z.J. Sun, Azo polymeric micelles designed for colon-targeted dimethyl fumarate delivery for colon cancer therapy, Acta Biomater 44 (2016) 323–331, doi:10.1016/j.actbio.2016.08.021.
[4] A. Bagheri, J. Yeow, H. Arandiyan, J. Xu, C. Boyer, M. Lim, Polymerization of a photocleavable monomer using visible light, Macromol. Rapid Commun. 37 (2016) 905–910, doi:10.1002/marc.201600127.
[5] S. Toughraï, V. Malinova, R. Masciadri, S. Menon, P. Tanner, C. Palivan, N. Bruns, W. Meier, Reduction-sensitive amphiphilic triblock copolymers self-assemble into stimuli-responsive micelles for drug delivery, Macromol. Biosci. 15 (2015) 481–489, doi:10.1002/mabi.201400400.
[6] C. Lin, H.L.H. Ng, W. Pan, H. Chen, G. Zhang, Z. Bian, A. Lu, Z. Yang, Exploring different strategies for efficient delivery of colorectal cancer therapy, Int. J. Mol. Sci. 16 (2015) 26936–26952, doi:10.3390/ijms161125995.
[7] T. Suma, J. Cui, M. Müllner, Y. Ju, J. Guo, M. Hu, F. Caruso, Generalizable strategy for engineering protein particles with pH-triggered disassembly and recoverable protein functionality, ACS Macro Lett. 4 (2015) 160–164, doi:10.1021/mz5007443.
[8] Y. Zhang, R. Wang, Y. Hua, R. Baumgartner, J. Cheng, Trigger-responsive poly(β-amino ester) hydrogels, ACS Macro Lett. 3 (2014) 693–697, doi:10.1021/mz500277j.
[9] X. Liang, F. Liu, V. Kozlovskaya, Z. Palchak, E. Kharlampieva, Thermoresponsive micelles from double LCST-poly(3-methyl-N-vinylcaprolactam) Block copolymers for cancer therapy, ACS Macro Lett. 4 (2015) 308–311, doi:10.1021/mz500832a.
[10] M. Yin, Y. Bao, X. Gao, Y. Wu, Y. Sun, X. Zhao, H. Xu, Z. Zhang, S. Tan, Redox/pH dual-sensitive hybrid micelles for targeting delivery and overcoming multidrug resistance of cancer, J. Mater. Chem. B 5 (2017) 2964–2978, doi:10.1039/c6tb03282f.

[11] L. Zha, Y. Zhang, W. Yang, S. Fu, Monodisperse temperature-sensitive microcontainers, Adv. Mater. 14 (2002) 1090–1092.
[12] P.F. Caponi, F.M. Winnik, R.V. Ulijn, Charge complementary enzymatic reconfigurable polymeric nanostructures, Soft Matter 8 (2012) 5127–5130, doi:10.1039/c2sm07460e.
[13] A.D. Wong, T.M. Güngör, E.R. Gillies, Multiresponsive azobenzene end-cap for self-immolative polymers, ACS Macro Lett. 3 (2014) 1191–1195, doi:10.1021/mz500613d.
[14] Z. Ma, R. Ma, X. Wang, J. Gao, Y. Zheng, Z. Sun, Enzyme and PH responsive 5-flurouracil (5-FU) loaded hydrogels based on olsalazine derivatives for colon-specific drug delivery, Eur. Polym. J. 118 (2019) 64–70, doi:10.1016/j.eurpolymj.2019.05.017.
[15] M. Naeem, W. Kim, J. Cao, Y. Jung, J.W. Yoo, Enzyme/pH dual sensitive polymeric nanoparticles for targeted drug delivery to the inflamed colon, Colloids Surf. B Biointerfaces 123 (2014) 271–278, doi:10.1016/j.colsurfb.2014.09.026.
[16] A.X. Gao, L. Liao, J.A. Johnson, Synthesis of acid-labile PEG and PEG-doxorubicin-conjugate nanoparticles via Brush-First ROMP, ACS Macro Lett. 3 (2014) 854–857, doi:10.1021/mz5004097.
[17] J. Zhou, H. Xu, Z. Tong, Y. Yang, G. Jiang, Photo/pH-controlled host–guest interaction between an azobenzene-containing block copolymer and water-soluble pillar[6]arene as a strategy to construct the “compound vesicles” for controlled drug delivery, Mater. Sci. Eng. C 89 (2018) 237–244, doi:10.1016/j.msec.2018.04.010.
[18] N. Feng, G. Han, J. Dong, H. Wu, Y. Zheng, G. Wang, Nanoparticle assembly of a photo- and pH-responsive random azobenzene copolymer, J. Colloid Interface Sci. 421 (2014) 15–21, doi:10.1016/j.jcis.2014.01.036.
[19] G. Wang, D. Yuan, T. Yuan, J. Dong, N. Feng, G. Han, A visible light responsive azobenzene-functionalized polymer: synthesis, self-assembly, and photoresponsive properties, J. Polym. Sci. Part A Polym. Chem. 53 (2015) 2768–2775, doi:10.1002/pola.27747.
[20] J. Wang, B. Wu, S. Li, Y. He, NIR light and enzyme dual stimuli-responsive amphiphilic diblock copolymer assemblies, J. Polym. Sci. Part A Polym. Chem. 55 (2017) 2450–2457, doi:10.1002/pola.28632.
[21] T. Yuan, J. Dong, G. Han, G. Wang, Polymer nanoparticles self-assembled from photo-, pH- and thermo-responsive azobenzene-functionalized PDMAEMA, RSC Adv. 6 (2016) 10904–10911, doi:10.1039/c5ra26894j.
[22] M. Billamboz, F. Mangin, N. Drillaud, C. Chevrin-Villette, E. Banaszak-Léonard, C. Len, Micellar catalysis using a photochromic surfactant: application to the pd-catalyzed tsuji-trost reaction in water, J. Org. Chem. 79 (2014) 493–500, doi:10.1021/jo401737t.
[23] R. Rajaganesh, A. Gopal, T.Mohan Das, A. Ajayaghosh, Synthesis and properties of amphiphilic photoresponsive gelators for aromatic solvents, Org. Lett. 14 (2012) 748–751, doi:10.1021/ol203294v.
[24] T. Ube, K. Takado, T. Ikeda, Photomobile materials with interpenetrating polymer networks composed of liquid-crystalline and amorphous polymers, J. Mater. Chem. C 3 (2015) 8006–8009, doi:10.1039/C5TC01489A.
[25] A. Franche, A. Fayeulle, L. Lins, M. Billamboz, I. Pezron, M. Deleu, E. Léonard, Amphiphilic azobenzenes: antibacterial activities and biophysical investigation of their interaction with bacterial membrane lipids, Bioorg. Chem. 94 (2020) 103399, doi:10.1016/j.bioorg.2019.103399.
[26] D.P. Ferris, Y.L. Zhao, N.M. Khashab, H.A. Khatib, J.F. Stoddart, J.I. Zink, Light-operated mechanized nanoparticles, J. Am. Chem. Soc. 131 (2009) 1686–1688, doi:10.1021/ja807798g.
[27] V.V. Jerca, F.A. Jerca, I. Rau, A.M. Manea, D.M. Vuluga, F. Kajzar, Advances in understanding the photoresponsive behavior of azobenzenes substituted with strong electron withdrawing groups, Opt. Mater. (Amst). 48 (2015) 160–164, doi:10.1016/j.optmat.2015.07.042.
[28] H.M.D. Bandara, S.C. Burdette, Photoisomerization in different classes of azobenzene, Chem. Soc. Rev. 41 (2012) 1809–1825, doi:10.1039/c1cs15179g.
[29] C. Boulègue, M. Löweneck, C. Renner, L. Moroder, Redox potential of azobenzene as an amino acid residue in peptides, ChemBioChem 8 (2007) 591–594, doi:10.1002/cbic.200600495.
[30] T. Eom, W. Yoo, S. Kim, A. Khan, Biologically activatable azobenzene polymers targeted at drug delivery and imaging applications, Biomaterials 185 (2018) 333–347, doi:10.1016/j.biomaterials.2018.09.020.
[31] W.X. Gu, Q.L. Li, H. Lu, L. Fang, Q. Chen, Y.W. Yang, H. Gao, Construction of stable polymeric vesicles based on azobenzene and beta-cyclodextrin grafted poly(glycerol methacrylate)s for potential applications in colon-specific drug delivery, Chem. Commun. 51 (2015) 4715–4718, doi:10.1039/c5cc00628g.
[32] Y. Zhou, M. Maiti, A. Sharma, M. Won, L. Yu, L.X. Miao, J. Shin, A. Podder, K.N. Bobba, J. Han, S. Bhuniya, J.S. Kim, Azo-based small molecular hypoxia responsive theranostic for tumor-specific imaging and therapy, J. Control. Release 288 (2018) 14–22, doi:10.1016/j.jconrel.2018.08.036.
[33] L.F. Kadem, M. Holz, K.G. Suana, Q. Li, C. Lamprecht, R. Herges, C. Selhuber-Unkel, Rapid reversible photoswitching of integrin-mediated adhesion at the single-cell level, Adv. Mater. 28 (2016) 1799–1802, doi:10.1002/adma.201504394.
[34] P. Gorde, S. Akole, A. Pingle, S. Wagh, Development of novel azobenzene diacetic acid allyl ester polymers for colon specific drug delivery, Am. J. PharmTech Res. 5 (2015) 243–254.
[35] S.H. Lee, E. Moroz, B. Castagner, J.C. Leroux, Activatable cell penetrating peptide-peptide nucleic acid conjugate via reduction of azobenzene PEG chains, J. Am. Chem. Soc. 136 (2014) 12868–12871, doi:10.1021/ja507547w.
[36] J. Rao, A. Khan, Enzyme sensitive synthetic polymer micelles based on the azobenzene motif, J. Am. Chem. Soc. 135 (2013) 14056–14059, doi:10.1021/ja407514z.
[37] A. Chevalier, P.-Y. Renard, A. Romieu, Azo-based fluorogenic probes for biosensing and bioimaging: recent advances and upcoming challenges, Chem.–Asian J. 12 (2017) 2008–2028, doi:10.1002/asia.201700682.
[38] Y.Y. Yang, M. Grammel, A.S. Raghavan, G. Charron, H.C. Hang, Comparative analysis of cleavable azobenzene-based affinity tags for bioorthogonal chemical proteomics, Chem. Biol. 17 (2010) 1212–1222, doi:10.1016/j.chembiol.2010.09.012.
[39] S.P. Kuruvilla, G. Tiruchinapally, M. ElAzzouny, M.E.H. ElSayed, N-acetylgalactosamine-targeted delivery of dendrimer-doxorubicin conjugates influences doxorubicin cytotoxicity and metabolic profile in hepatic cancer cells, Adv. Healthc. Mater. 6 (2017) 1–15, doi:10.1002/adhm.201601046.
[40] C. Le Berre, G. Roda, M. Nedeljkovic Protic, S. Danese, L. Peyrin-Biroulet, Modern use of 5-aminosalicylic acid compounds for ulcerative colitis, Expert Opin. Biol. Ther. 20 (2020) 363–378, doi:10.1080/14712598.2019.1666101.
[41] H. Shahdadi Sardo, F. Saremnejad, S. Bagheri, A. Akhgari, H. Afrasiabi Garekani, F. Sadeghi, A review on 5-aminosalicylic acid colon-targeted oral drug delivery systems, Int. J. Pharm. 558 (2019) 367–379, doi:10.1016/j.ijpharm.2019.01.022.
[42] D. Nagpal, R. Singh, N. Gairola, S. Bodhankar, S. Dhaneshwar, Mutual azo prodrug of 5-aminosalicylic acid for colon targeted drug delivery: synthesis, kinetic studies and pharmacological evaluation, Indian J. Pharm. Sci. 68 (2006) 171–178, doi:10.4103/0250-474x.25710.
[43] Y. Yan, J. Sun, X. Xie, P. Wang, Y. Sun, Y. Dong, J. Xing, Colon-targeting mutual prodrugs of 5-aminosalicylic acid and butyrate for the treatment of ulcerative colitis, RSC Adv. 8 (2018) 2561–2574, doi:10.1039/c7ra13011b.
[44] S.S. Dhaneshwar, N. Gairola, M. Kandpal, G. Vadnerkar, L. Bhatt, B. Rathi, S.S. Kadam, Synthesis, kinetic studies and pharmacological evaluation of mutual azo prodrugs of 5-aminosalicylic acid for colon-specific drug delivery in inflammatory bowel disease, Eur. J. Med. Chem. 44 (2009) 3922–3929, doi:10.1016/j.ejmech.2009.04.018.
[45] J. Nam, W. Kim, S. Lee, S. Jeong, J.W. Yoo, M.S. Kim, Y. Jung, Dextran-5-(4-ethoxycarbonylphenylazo)salicylic acid ester, a polymeric colon-specific prodrug releasing 5-aminosalicylic acid and benzocaine, ameliorates TNBS-induced rat colitis, J. Drug Target 24 (2016) 468–474, doi:10.3109/1061186X.2015.1087528.
[46] M. Mahkam, Novel pH-sensitive hydrogels for colon-specific drug delivery, Drug Deliv. 17 (2010) 158–163, doi:10.3109/10717541003604908.
[47] S.Q. Gao, Z.R. Lu, B. Petri, P. Kopečková, J. Kopeček, Colon-specific 9-aminocamptothecin-HPMA copolymer conjugates containing a 1,6-elimination spacer, J. Control. Release 110 (2006) 323–331, doi:10.1016/j.jconrel.2005.10.004.
[48] T. Eom, W. Yoo, Y.D. Lee, J.H. Park, Y. Choe, J. Bang, S. Kim, A. Khan, An activatable anticancer polymer-drug conjugate based on the self-immolative azobenzene motif, J. Mater. Chem. B 5 (2017) 4574–4578, doi:10.1039/c7tb01250k.
[49] M. Akram, L. Wang, H. Yu, W.A. Amer, H. Khalid, N.M. Abbasi, Y. Chen, M.Saleem Zain-Ul-Abdin, R. Tong, Polyphophazenes as anti-cancer drug carriers: from synthesis to application, Prog. Polym. Sci. 39 (2014) 1987–2009, doi:10.1016/j.progpolymsci.2014.07.009.
[50] R.S. Ullah, L. Wang, H. Yu, N.M. Abbasi, M. Akram, Z. Ul-Abdin, M. Saleem, M. Haroon, R.U. Khan, Synthesis of polyphosphazenes with different side groups and various tactics for drug delivery, RSC Adv. 7 (2017) 23363–23391, doi:10.1039/c6ra27103k.
[51] M. Canevari, I. Castagliuolo, P. Brun, M. Cardin, M. Schiavon, G. Pasut, F.M. Veronese, Poly(ethylene glycol)-mesalazine conjugate for colon specific delivery, Int. J. Pharm. 368 (2009) 171–177, doi:10.1016/j.ijpharm.2008.09.058.
[52] E.-R. Kenawy, S.S. Al-Deyab, M.H. El-Newehy, Controlled release of 5-aminosalicylic acid (5-ASA) from new biodegradable polyurethanes, Molecules 15 (2010) 2257–2268, doi:10.3390/molecules15042257.
[53] K. Hakkou, I. Molina-Pinilla, C. Rangel-Núñez, A. Suárez-Cruz, E. Pajuelo, M. Bueno-Martínez, Synthesis of novel (bio) degradable linear azo polymers conjugated with olsalazine, Polym. Degrad. Stab. 167 (2019) 302–312, doi:10.1016/j.polymdegradstab.2019.07.013.
[54] M. Saffran, G. Kumar, C. Savariar, J. Burnham, F. Williams, D. Neckers, A new approach to the oral administration of insulin and other peptide drugs, Science (80-.) 233 (1986) 1081–1084, doi:10.1126/science.3526553.
[55] H. Mutlu, C. Barner-Kowollik, Green chain-shattering polymers based on a self-immolative azobenzene motif, Polym. Chem. 7 (2016) 2272–2279, doi:10.1039/c5py01937k.
[56] H. Lei, M. Mo, Y. He, Y. Wu, W. Zhu, L. Wu, Bioactivatable reductive cleavage of azobenzene for controlling functional dumbbell oligodeoxynucleotides, Bioorg. Chem. (2019) 91, doi:10.1016/j.bioorg.2019.103106.
[57] R.L. Singh, P.K. Singh, R.P. Singh, Enzymatic decolorization and degradation of azo dyes—a review, Int. Biodeterior. Biodegrad. 104 (2015) 21–31, doi:10.1016/j.ibiod.2015.04.027.
[58] A.D. Wong, A.L. Prinzen, E.R. Gillies, Poly(ester amide)s with pendant azobenzenes: multi-responsive self-immolative moieties for modulating polymer assemblies, Polym. Chem. 7 (2016) 1871–1881, doi:10.1039/c5py01824b.
[59] W.M. Koppes, J.S. Moran, J.C. Oxley, J.L. Smith, Azo bond hydrogenation with hydrazine, R-NHNH2, and hydrazobenzene, Tetrahedron Lett. 49 (2008) 3234–3237, doi:10.1016/j.tetlet.2008.03.083.
[60] M.W. Jones, G. Mantovani, C.A. Blindauer, S.M. Ryan, X. Wang, D.J. Brayden, D.M. Haddleton, Direct peptide bioconjugation/PEGylation at tyrosine with linear and branched polymeric diazonium salts, J. Am. Chem. Soc. 134 (2012) 7406–7413, doi:10.1021/ja211855q.

[61] G. Leriche, G. Budin, L. Brino, A. Wagner, Optimization of the azobenzene scaffold for reductive cleavage by dithionite; development of an azobenzene cleavable linker for proteomic applications, European J. Org. Chem. 2010 (2010) 4360–4364, doi:10.1002/ejoc.201000546.
[62] C.L. Folcia, I. Alonso, J. Ortega, J. Etxebarria, I. Pintre, M.B. Ros, Achiral bent-core liquid crystals with azo and azoxy linkages: structural and nonlinear optical properties and photoisomerization, Chem. Mater. 18 (2006) 4617–4626, doi:10.1021/cm060256p.
[63] D. Zhao, D. Ouyang, M. Jiang, Y. Liao, H. Peng, X. Xie, Photomodulated Electro-optical Response in Self-Supporting Liquid Crystalline Physical Gels, American Chemical Society, 2018, doi:10.1021/acs.langmuir.8b01031.
[64] S. Asada, A. Nito, Y. Miyagi, J. Ishida, Y. Obora, F. Sanda, Sonogashira-Hagihara and Mizoroki-Heck coupling polymerizations catalyzed by Pd nanoclusters, Macromolecules 50 (2017) 4083–4087, doi:10.1021/acs.macromol.7b00779.
[65] K. Hakkou, M. Bueno-Martínez, I. Molina-Pinilla, J.A. Galbis, Degradable poly(ester triazole)s based on renewable resources, J. Polym. Sci. Part A Polym. Chem. 53 (2015) 2481–2493, doi:10.1002/pola.27710.
[66] D. Braun, H. Chedron, W. Kern, Praktikum Der Makromolekularen Organischen Chemie, Heidelberg, 1966.
[67] C. Rangel-Núñez, C. Ramírez-Trujillo, K. Hakkou, A. Suárez-Cruz, I. Molina-Pinilla, M. Bueno-Martínez, Regiospecific *vs.* non regiospecific click azide-alkyne polymerization: *in vitro* study of water-soluble antibacterial poly(amide aminotriazole)s, Mater. Sci. Eng. C 125 (2021) 112113, doi:10.1016/j.msec.2021.112113.
[68] A. Abbott, Biology's new dimension, Nature 424 (2003) 870–872, doi:10.1038/424870A.